CARBON 80 (2014) 396–404

Available at www.sciencedirect.com

ScienceDirect

journal homepage: www.elsevier.com/locate/carbon

Highly stretchable conductors and piezocapacitive strain gauges based on simple contact-transfer patterning of carbon nanotube forests

Ung-Hui Shin [a], *Dong-Wook Jeong* [b], *Sang-Min Park* [a], *Soo-Hyung Kim* [a,b,c], *Hyung Woo Lee* [b,d,*], *Jong-Man Kim* [a,b,c,*]

[a] *Department of Advanced Circuit Interconnection, Pusan National University, Busan 609-735, Republic of Korea*
[b] *Department of Nano Fusion Technology, Pusan National University, Busan 609-735, Republic of Korea*
[c] *Department of Nanomechatronics Engineering, Pusan National University, Busan 609-735, Republic of Korea*
[d] *Department of Nanomaterials Engineering, Pusan National University, Busan 609-735, Republic of Korea*

ARTICLE INFO

Article history:
Received 16 June 2014
Accepted 21 August 2014
Available online 28 August 2014

ABSTRACT

Three-dimensionally interconnected carbon nanotubes (CNTs) in a vertically aligned CNT (*v*CNT) forest are potentially desirable for retaining their electrical functionality under various elastic deformations after being incorporated into elastomeric materials. Here, we report a class of highly stretchable and reliable elastic conductors based on the elastomer-infiltrated *v*CNT forest with micro-patternability enabled by a facile and accurate contact-transfer patterning approach. The stretchable conductors show electrical and mechanical robustness over a wide range of tensile strains of up to ~450% and fully-stabilized response characteristics after some pre-conditioning. In addition, the electrical performance of the stretchable conductors is also found to be fairly retained without significant degradation in response to other types of elastic deformations such as bending, twisting, and folding. In this way, we demonstrate a piezocapacitive strain gauge that can measure large tensile strains as high as ~150% with superior linearity, sustainability, and reversibility of the resultant capacitive responses. We show that the strain gauges can be used to monitor large-scale static and dynamic motions of human parts in real time.

1. Introduction

Elastic conductors play an important role in a new class of stretchable electronics as electrodes and interconnects that can retain their performance (e.g., conductivity) without significant degradation under various elastic deformations such as stretching, bending, twisting, folding and so on. A number of conductive materials, such as metallic thin-films configured into waves or buckles [1–9], metallic nanowires (NWs) [10–15], graphene [16–18], and carbon nanotubes (CNTs) [19–37] have been used to fabricate such elastic conductors by introducing electrical conductivity to elastic materials such as polydimethylsiloxane (PDMS). CNTs in particular have gained great attention as one of the most important con-

* *Corresponding authors:* Address: Department of Nano Fusion Technology, Pusan National University, Busan 609-735, Republic of Korea. Fax: +82 51 514 2358 (H.W. Lee). Address: Department of Advanced Circuit Interconnection, Pusan National University, Busan 609-735, Republic of Korea. Fax: +82 55 350 5289 (J.-M. Kim).
E-mail addresses: lhw2010@pusan.ac.kr (H.W. Lee), jongkim@pusan.ac.kr (J.-M. Kim).
http://dx.doi.org/10.1016/j.carbon.2014.08.079
0008-6223/

ductive materials in stretchable electronics due to advantages such as high aspect ratio, good electrical conductivity, and mechanical robustness. Therefore, a variety of attempts have been carried out to realize CNT-based elastic conductors, such as conductive polymer nanocomposites prepared by embedding CNTs into a polymer matrix [19–26], polymer-infiltrated CNT forests or networks [27–29], CNT films coated or transferred onto elastic substrates [30–33], and CNT ribbons or fibers stacked on elastic substrates [34–37]. The micropatternability of CNT-based elastic materials (CEMs) is also a critical issue for integration with stretchable devices. Shadow masks have been most widely used thus far to fabricate micrometer- or millimeter-scale patterns of CEMs [29–32]. For example, CNTs dispersed in solution can be patterned directly on polymer substrates based on a spray coating process with a shadow mask [30,31]. CNT-inlaid elastomeric patterns can also be obtained by spray coating on a glass substrate with a shadow mask and subsequently transferring the patterns to elastomeric materials through a typical replication process [29]. Vacuum-filtered CNT percolation networks can be patterned on a silicone substrate treated selectively with oxygen plasma based on a shadow mask through a direct contact-and-transfer method [32]. A shadow mask can also be used to fabricate the CNT/polymer nanocomposite patterns by squeezing the composited material into opening area of the shadow mask [24,25]. Although patterning processes based on shadow masks are quite straightforward, they generally suffer from inferior critical dimension (CD) control. High-precision shadow masks such as laser-ablated thin plastic films can be used to enhance the resolution of resultant composite patterns [25]. The main drawbacks of this approach are the requirements for complex and expensive setups to prepare shadow masks with accurate pattern holes. Moreover, the fabrication might become more time consuming and inefficient because a specialized process must be employed repeatedly for individual designs and each new layout. Another solution is to use photolithographically-defined polymer masks instead of the shadow masks. Although more accurate patterning of CEMs is possible in this approach thanks to well-established photolithographic techniques, additional processes are inevitable, such as manual removal of excessive nanocomposite after squeezing by a razor blade, resulting in the complexity in fabrication [26].

Here, we report an alternative method for demonstrating a highly stretchable and patternable elastic conductor based on a vertically aligned CNT (vCNT) forest and simple contact-transfer patterning approach. The vCNT forest is a promising conductive pathway for stretchable conductors because of the three-dimensional (3D) interconnections among the CNTs in the forest. In addition, the proposed contact-transfer patterning technique allows for the simple and accurate fabrication of micro-scale CNT forest patterns in arbitrary shapes. After infiltrating highly elastic polymer, the CNT forest patterns can behave as a stretchable conductor that is robust against various elastic deformations. In this way, we demonstrate a piezocapacitive strain gauge based on the CNT forest elastic electrodes and intermediate elastic insulating layer, ensuring highly linear, stable, and reversible responses for tensile strain up to 150%. Finally, the practical usability of the proposed strain gauges was demonstrated by monitoring human motions in real time after integrating the devices onto parts of the body (the finger and knee joints) undergoing large bending deformations.

2. Experimental details

2.1. Synthesis of vertically aligned carbon nanotube (vCNT) forest

The vCNT forest used as a conducting medium in this study was grown on a four-inch oxidized silicon substrate deposited with a supporting catalytic metal layer of iron (Fe) and a barrier layer of alumina (Al_2O_3) by a thermal CVD process. In detail, ~10-nm-thick Al_2O_3 and ~2-nm-thick Fe layers were sequentially deposited on a cleaned oxidized silicon wafer by atomic layer deposition (ALD) and electron-beam evaporation processes, respectively. The catalyst-deposited samples were then placed in a CVD chamber under a hydrogen (H_2) flow rate of 700 sccm, a pressure of 80 mbar, and a temperature of 625 °C for 30 s to establish the catalytic islands as a seed for growing CNTs. CNT growth was subsequently carried out by adding 50 sccm of ethyne (C_2H_2) gas. For the growth, the pressure and temperature of the chamber were kept at 80 mbar and 675 °C, respectively.

2.2. Fabrication of stretchable conductors and strain gauges

The vCNT conductor patterns were first defined by removing the unnecessary parts of the vCNT forest by a selective contact-transfer technique using a PDMS stamp, which was prepared by standard soft-lithographic molding and replication processes. For this, a ~70-μm-thick photoresist (PR, JSR-THB-151N) mold was first patterned on a cleaned four-inch silicon wafer using a photolithography process. Next, liquid PDMS (with a 20:1 weight ratio of the base polymer to the curing agent) was poured onto the mold substrate, followed by curing at 70 °C for ~20 min. The curing time was optimized to make the PDMS surface sticky since the sticky surface of the elastomeric stamp facilitates easy contact-transfer patterning. The elastomeric stamp was finally prepared by peeling off the solidified PDMS from the mold substrate. The prepared PDMS stamp was then brought into contact with the vCNT forest using a manual *xyz*-stage. When lifted off the stamp, unnecessary vCNT parts in the area of physical contact were selectively removed, leaving the desired vCNT conductor patterns on the donor substrate. After that, the vCNT conductor patterns remaining on the donor substrate were transferred entirely onto the Ecoflex substrate (with a 1:1 weight ratio of the base polymer to the curing agent) through the contact-transfer technique. The vCNT forests patterned on the Ecoflex substrate were then infiltrated with a liquid Ecoflex solution, which was diluted with a volatile solvent (toluene) in a weight ratio of 5:1, by a drop-casting process in order to assure the mechanical robustness and reversible behavior of the elastic conductors without severe performance degradation even under repetitive operation. After fully evaporating the volatile solvent at 70 °C for 2 h, the fabricated elastic vCNT conductor was packaged through

drop-casting a protective liquid Ecoflex and subsequent curing at 70 °C for 2 h.

To demonstrate a piezocapacitive strain gauge, two elastic vCNT electrodes were first prepared by the aforementioned fabrication procedures, except for the final curing step of the protective Ecoflex layer. The two stretchable electrodes prepared with uncured Ecoflex layers were then aligned carefully to allow for an overlapping area of $1 \times 1\ cm^2$, and then thermally cured at 70 °C for 2 h under slightly pressurized conditions to ensure strong bonding between the two electrodes for mechanical and electrical stability.

2.3. Characterization

An automatic test stand (JSV-H1000, JISC) equipped with a push–pull force gauge (H-10, JISC) was used to apply tensile strain to the vCNT conductor clamped to the stage at both ends, and a digital multimeter (U1253B, Agilent Technologies) interfaced with a computer through RS-232 data cable was employed to measure and record the electrical resistance with respect to the applied strain in real time.

The capacitive responses of the fabricated strain gauge were measured using an LCR meter (model-6375, Microtest) connected to a computer with a data cable, while applying the external forces by a motorized stage equipped with a force gauge.

3. Results and discussion

3.1. vCNT forest

In general, CNTs consist of metallic and semiconducting nanotubes as grown by chemical vapor deposition (CVD). Even though one third of the whole nanotubes, the metallic

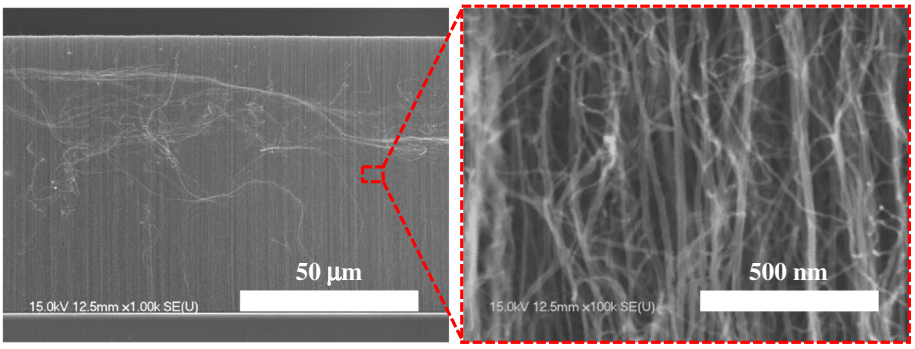

Fig. 1 – Cross-sectional SEM image of the vertically aligned carbon nanotube (vCNT) forest prepared by thermal CVD process (the magnified SEM image clearly indicates three-dimensionally interconnected CNTs in the forest). (A color version of this figure can be viewed online.)

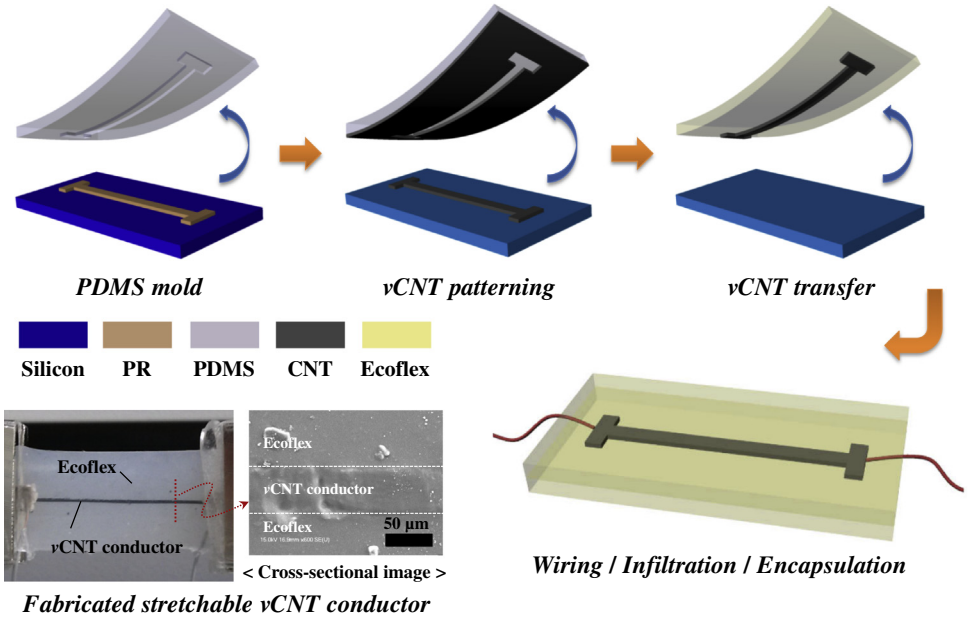

Fig. 2 – Fabrication procedures of the stretchable vCNT conductors based on simple two-step contact-transfer patterning technique (inset figures: fabricated stretchable vCNT conductor and cross-sectional SEM image). (A color version of this figure can be viewed online.)

CNTs are the dominant paths in current flow. Fig. 1 shows a scanning electron microscope (SEM) image indicating a cross-sectional profile of the prepared vCNT forest. In particular, it can clearly be seen that the CNTs formed 3D conductive networks by being entangled with each other, as shown in the magnified SEM image in Fig. 1. This provides clear evidence of the fact that the vCNT forest is one of the most efficient candidates for conducting materials in stretchable electronics.

3.2. *vCNT forest-based stretchable conductors*

Thus far, PDMS has been the material most widely used for stretchable substrates due to its good flexibility and easy accessibility. Nevertheless, the stretchability of PDMS-based elastic conductors is typically restricted to ~100% strain or less, which might originate from the fracture limit of PDMS. In this study, Ecoflex, an extremely soft elastomeric material, was employed to extend the usable strain range by overcoming the limits of the PDMS. Micro-patterning of the proposed elastic conductors was achieved simply by transferring the necessary portions of the vCNT forest onto the Ecoflex substrate by a two-step contact-transfer patterning method, as illustrated schematically in Fig. 2.

The proposed two-step contact-transfer approach can be useful alternative for fabricating CNT-based elastic conductors by enabling the preparation of arbitrary shapes of the vCNT forest patterns, as shown in Fig. S1 (see Supporting information). The fabrication method ensures two key merits of high patterning accuracy and process simplicity, because the micro-patterning of the vCNT conductors is based on well-established photolithography and simple contact-transfer methods. Based on the two-step contact-transfer approach, a ribbon-shaped vCNT conductor was successfully prepared, as shown in the digital and cross-sectional SEM images in Fig. 2. In particular, the height of the fabricated

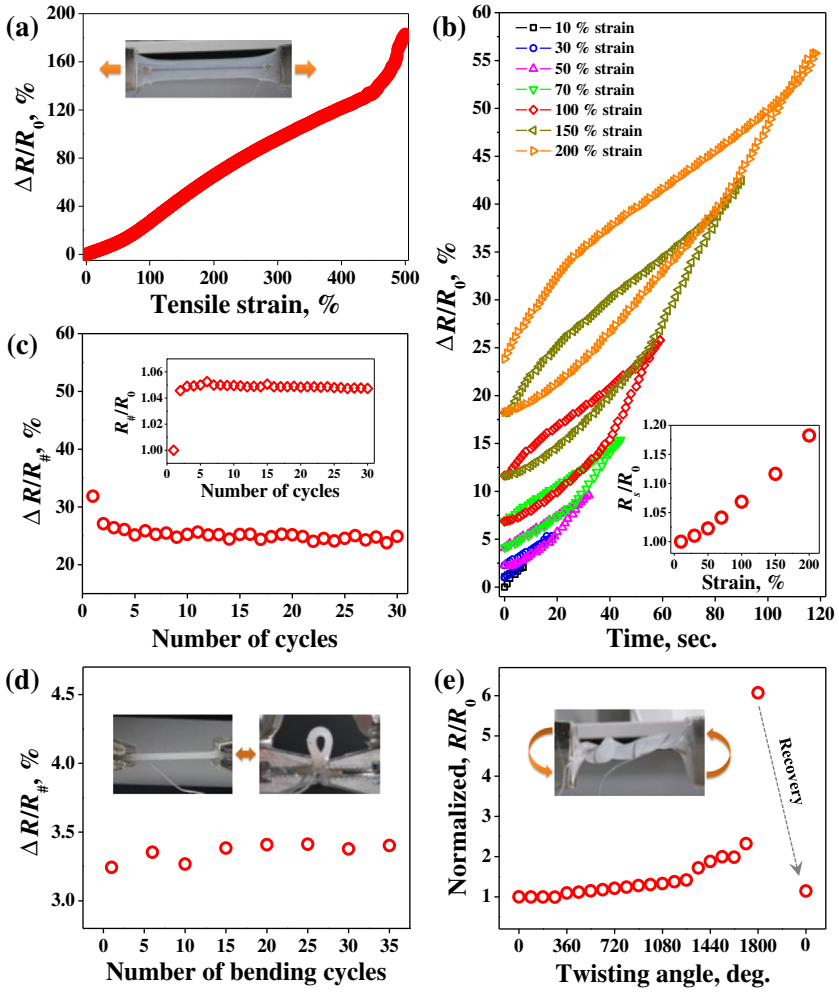

Fig. 3 – Performance evaluations of the stretchable vCNT conductors. (a) Resistance change ratio ($\Delta R/R_0$) as a function of applied tensile strain up to 500%. (b) $\Delta R/R_0$ under continuous strain loading and unloading with increased maximum strain ranging from 10% to 200%. (c) Resistance change ratio for each stretching/releasing cycle with a maximum tensile strain of 200% (inset: normalized initial resistance for each cycle with respect to starting resistance (R_0)). (d) Resistance change ratio under cyclic bending deformations (minimum bending radius: ~2 mm). (e) Normalized resistance under twisting deformations up to 1800 degrees (5 turns). (A color version of this figure can be viewed online.)

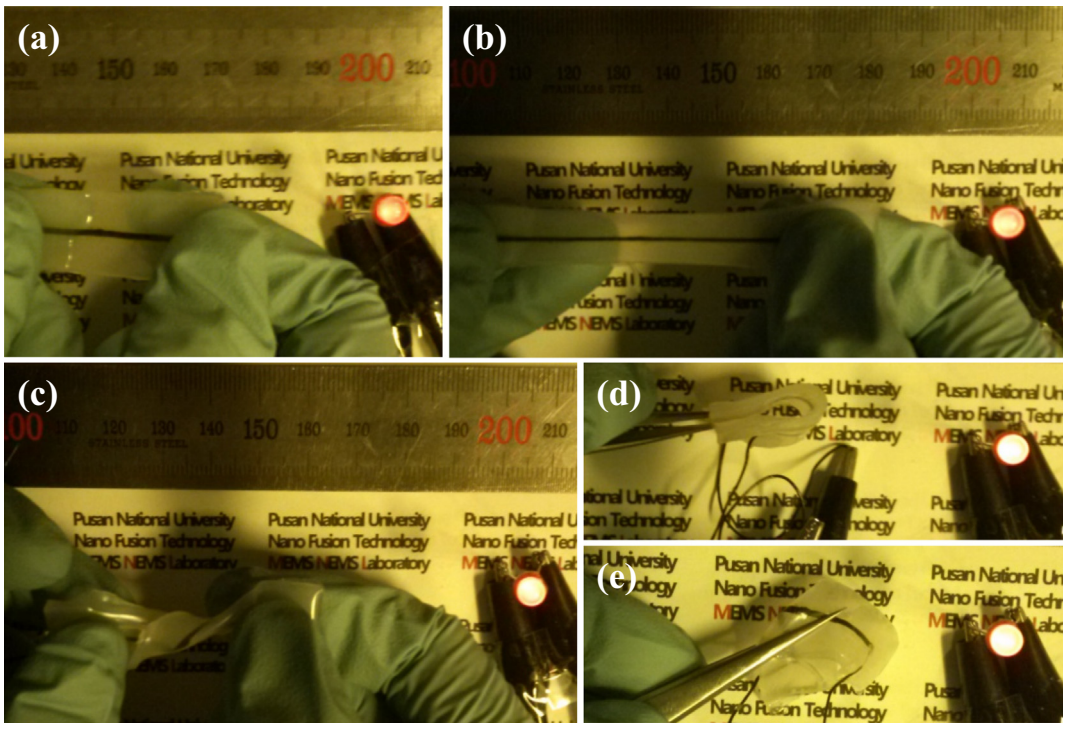

Fig. 4 – LED demonstrations under various elastic deformations with applied turn-on voltage of 4 V. (a) Initial state. (b) Under stretching. (c) Under twisting. (d) Under bending. (e) Under folding. (A color version of this figure can be viewed online.)

υCNT conductor was maintained similarly compared to that of as-grown forest, which may imply that vertical architecture of the CNTs is also fairly retained even after experiencing the process.

The electrical performance of the fabricated υCNT-based elastic conductors was first characterized by observing the strain-dependent electrical resistance using a two-probe technique under stretching deformation. Fig. 3(a) shows the resistance change ratio ($\Delta R/R_0$) of the υCNT conductor as a function of the applied tensile strain up to 500% with a constant loading speed of 5 mm/min. The resistance change ratio was increased linearly with a slope of ~0.3 as the applied tensile strain increased up to ~450%. This means that 3D conductive networks of the υCNT forest in the Ecoflex matrix could be deformed gradually in a stable manner, indicating predictable electrical performance even under relatively high strain. In addition, the retention of the electrical performance of the device under high strain is probably attributed to the fact that many of contact junctions among the υCNTs entangled densely in elastomer matrix still maintain electrical connection upon stretching due to "contact junction shift" [38], as illustrated schematically in Fig. S2 (see Supporting information). Electrical failure of the fabricated υCNT conductor was observed at ~450% strain, at which the resistance was unstably increased with a very steep slope, as shown in Fig. 3(a). The sudden increase in electrical resistance might have originated from loss of a number of conductive networks among the υCNTs due to the application of tensile strain higher than the critical value that can retain fairly stable electrical performance in response to stretching deformations.

Fig. 3(b) presents the change in resistance under continuous loading (stretched to maximum strain) and unloading (released to 0% strain), with the increased maximum strain ranging from 10% to 200% having a constant loading speed of 12 mm/min. Although the tendency of the change in resistance with respect to the applied strain is similar to the result in Fig. 3(a), the resistance did not return perfectly to its starting value even when the applied strain was fully removed to 0% at each stage, as shown in Fig. 3(b). This hysteretic electrical behavior of the υCNT conductor at each stretching/releasing stage was probably due to the increment of its resistance from several reasons. Some 3D electrical networks in the υCNT forest have been broken when the υCNT conductor was exposed to tensile strain. In addition, interfacial contacts between neighboring υCNTs could be subjected to change in the direction of decreasing contact areas after experiencing such strain level, even though the υCNT conductor physically returned to its original length. This might have led to a resistance increase in the released state for each stage with respect to the unstrained value. In addition, the starting resistance (R_s) at each stage was increased gradually with increasing maximum strain (inset of Fig. 3(b)). This means that the υCNTs undergo more events that can irrecoverably deform the υCNT networks under higher strain loading conditions. Nonetheless, the resistance change was found to be highly reversible in the low strain range (up to ~50% strain), indicating low hysteresis less than 5% with respect to the initial resistance (R_0). In addition, even with the application of high strain (200%), the υCNT conductor exhibits an excellent reversibility after a few stretching/releasing cycles, as shown in Fig. 3(c) (where $R_\#$ means the initial resistance value for each cycle.). It should be noted that the initial resistance was increased ~16.2% compared to the case in Fig. 3(b), because the υCNT conductor was previously exposed to

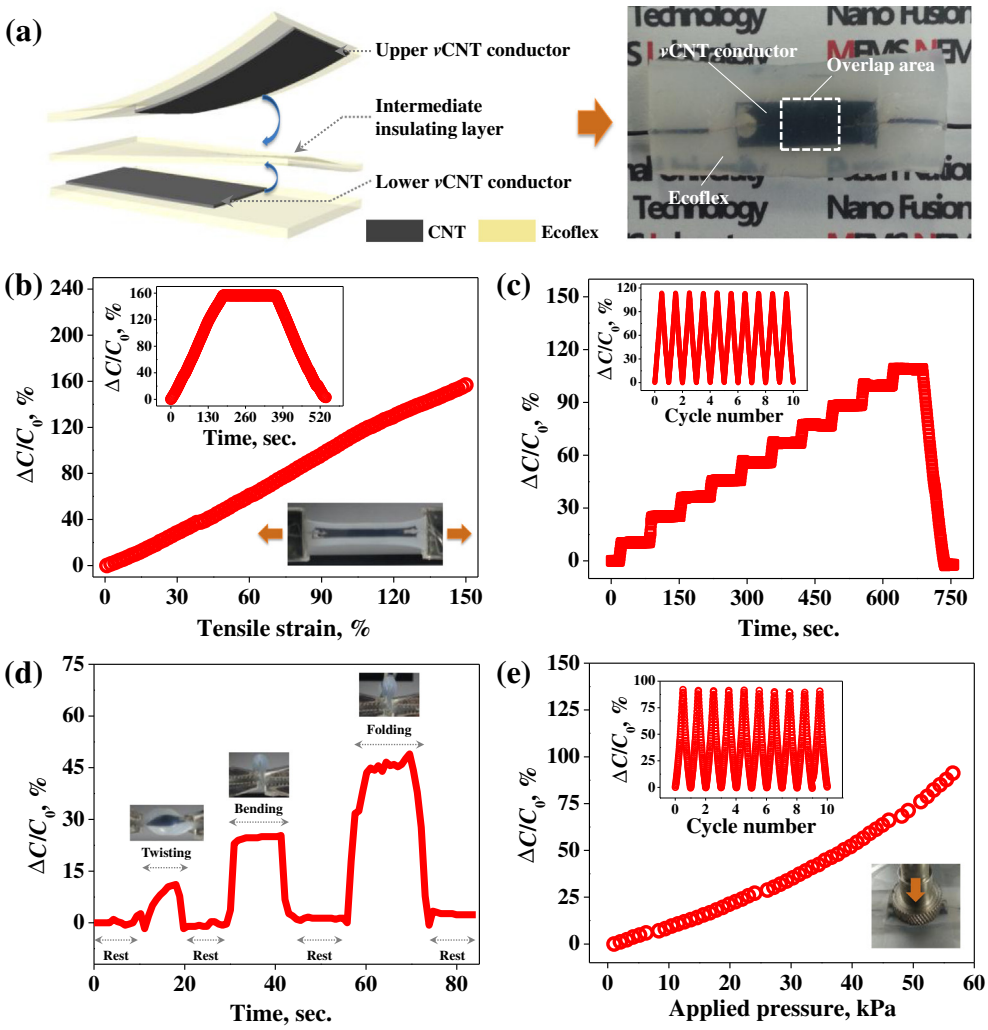

Fig. 5 – Performance evaluations of the elastic piezocapacitive strain gauge. (a) Schematic illustration of the strain gauge architecture and fabricated device. (b) Capacitance change ratio ($\Delta C/C_0$) under applied tensile strain up to 150% (inset: $\Delta C/C_0$ due to successive operations (strain loading → holding → strain unloading)). (c) $\Delta C/C_0$ under stepwise application of tensile strain (increased by 10% for each step) with a holding duration of ~1 min up to 100% (inset: cyclic capacitive responses with applied maximum strain of 100%). (d) $\Delta C/C_0$ under other types of elastic deformations. (e) $\Delta C/C_0$ under applied normal pressure up to ~56.5 kPa (inset: cyclic capacitive responses with applied maximum pressure of ~56.5 kPa). (A color version of this figure can be viewed online.)

200% strain, which resulted in lower resistance change ratio under the same strain loading (200%). The resistance change ratio became almost constant while maintaining small deviations less than 2.5% for each cycle after the fifth stretching/releasing cycle. This was probably attributed mainly to the stabilization in the released state (inset of Fig. 3(c)), which means that the νCNTs in the Ecoflex matrix physically reached the most stable state after the initial conditioning phase.

Further, the response characteristics of the νCNT conductors to other types of deformations, such as bending and twisting, were also investigated. Fig. 3(d) shows the resistance change of the fabricated νCNT conductor due to the applied cyclic bending deformations under a bending radius of ~2 mm. The resultant resistance change remained almost constant only within the range of 3.2–3.4% for each bending cycle. In addition, the νCNT conductor was also tested under severe twisting deformations of up to 1800 degrees (5 turns). The change in electrical resistance was found to be relatively insensitive to the applied twisting deformation by ~1080 degrees (a ~33% increase with respect to the untwisted resistance), as shown in Fig. 3(e). At 1800 degrees, a considerable increase of the resistance was observed, which may have been dominantly due to the presumable physical damage to the parts exposed to the largest stress under the extreme twisting. Nevertheless, the resistance of the νCNT conductor returned to the slightly higher value (~14% higher) compared to the untwisted state when the applied twisting deformation was fully released.

As a demonstration for practical applicability, the electrical characteristics of a simple light-emitting diode (LED) circuit integrated with the fabricated νCNT conductor under

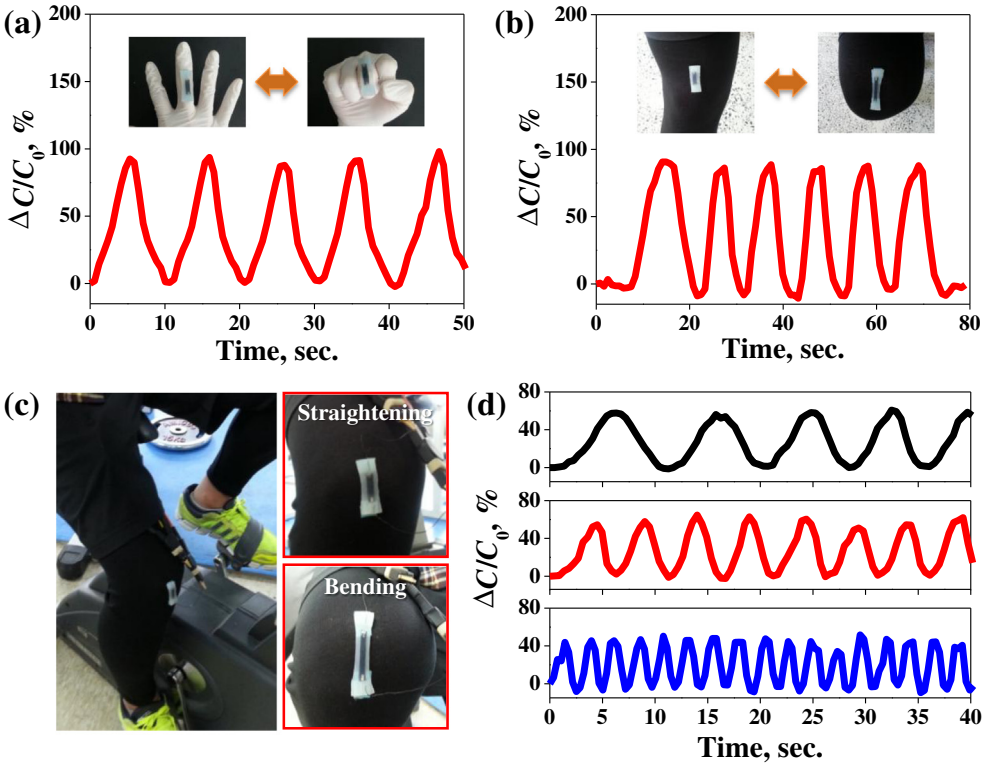

Fig. 6 – Potential demonstrations of the elastic piezocapacitive strain gauge integrated on human parts. (a, b) $\Delta C/C_0$ under simple bending and straightening motions of finger and knee, respectively. (c) Photographs of the strain gauge mounted on human knee during operating an exercise bike with close-up views of the device at the highest (knee bending) and lowest positions (knee straightening) of the pedal. (d) $\Delta C/C_0$ measured during operating the machine with different pedaling speeds. (A color version of this figure can be viewed online.)

various elastic deformations were investigated. The light intensity of the LED with the applied turn-on voltage of 4 V was almost retained without significant change, even when the υCNT conductor was subjected to stretching, twisting, bending, and folding deformations, as shown in Fig. 4. These experimental observations show the feasibility for the proposed υCNT conductor to be operated well in applications even under various elastic deformations while maintaining the stable electrical performance.

3.3. *Piezocapacitive elastic strain gauges*

Based on the υCNT conductors, a highly elastic piezocapacitive strain gauge capable of detecting the external forces by measuring a strain-dependent change in electrical capacitance was successfully demonstrated, as shown in Fig. 5. The strain gauge consists of two stretchable υCNT electrodes prepared by the aforementioned fabrication technique, with the elastomeric insulating layer between the two electrodes, as shown in Fig. 5(a). In the proposed piezocapacitive strain gauge, the protective Ecoflex layers act both as electrically insulating layers in between the two stretchable electrodes and bonding layers to form a parallel-plate capacitor.

Fig. 5(b) shows the capacitance change ratio ($\Delta C/C_0$) of the fabricated strain gauge with respect to the applied tensile strain up to 150%. The capacitance increased linearly as the gap distance between the two electrodes decreased under the applied tensile strain. In this way, a gauge factor (*GF*, $\Delta C/C_0/\varepsilon$) of ~1 was obtained and retained stably during holding for 3 min at 150% tensile strain, as shown in inset in Fig. 5(b). The performance stability of the strain gauge was further examined by observing its gauging properties under stepwise tensile strains up to 100% of strain (stretching first by 10% at a speed of 12 mm/min and subsequent holding for ~1 min). The *GF*s obtained from each stage were almost 1, and were also retained well without any fluctuation for each holding-duration, as shown in Fig. 5(c). The inset in Fig. 5(c) also indicates reliable sensor responses under repetitive stretching/releasing cycles, showing excellent reversibility. The sensor responses for other types of deformations such as twisting, bending, and folding were also found to be fully reversible. The capacitance in each deformed state was returned to its original value without any hysteretic behavior when all the applied deformations were fully released, as shown in Fig. 5(d).

All the experiments clearly indicate that the proposed piezocapacitive strain gauge is highly applicable to practical applications owing to its remarkably stable and reliable performance. In principle, the piezocapacitive elastic strain gauge can also react with pressure applied perpendicular to the device. The linear and reversible change in capacitance of the fabricated strain gauge was also observed with the application of a normal compressive force of up to ~10 N (corresponding to ~56.5 kPa in pressure), as shown in Fig. 5(e).

To demonstrate the potential of the piezocapacitive strain gauges capable of reacting with high strains ensuring both the mechanical robustness and electrical stability in practical applications, we integrated them onto parts of the body (the finger and knee joints), which usually experience large bending motions. Fig. 6(a) and (b) show the capacitive responses ($\Delta C/C_0$) of the fabricated devices under repetitive simple bending/straightening motions of the finger and knee, respectively, after mounting the devices on the joint regions. In both situations, the resultant changes in capacitance were quite uniform under similar levels of bending at each bending/straightening cycle, revealing high reversibility.

Further tests were carried out to explore the ability to sense dynamic motions of body parts by operating an exercise bike with the fabricated device attached to the knee joint, as shown in Fig. 6(c). Upon operating the machine, the sensor mounted on the knee joint experiences repetitive stretching and releasing states depending on the knee motions. Thus the continuous motions of the human knee can be detected as continuous changes in capacitance of the device. The corresponding capacitance changes are provided in Fig. 6(d). The maximum changes in the capacitance of the device were measured when a pedal of the bike was at the highest position (corresponding to knee bending), while the capacitance changes were minimized in the lowest position of the pedal (corresponding to knee straightening) during the operations. The capacitive responses of the device were quite reversible and stable without large deviations for each operating cycle. In addition, different pedaling speeds on the machine were also detectable in real time using the fabricated device. With increasing pedaling speed (and more rapid knee motion), the period of the capacitive response became shorter, and vice versa, as shown in Fig. 6(d). These demonstrations clearly suggest that the proposed piezocapacitive strain gauges have the possibility to be employed in practical sensing applications dealing with large strain deformations such as large-scale human motions, owing to their wide detectable range of strains of up to 150% and reliable mechanical and electrical functionalities.

4. Conclusions

In this work, we present highly stretchable conductors by incorporating a conductive υCNT forest into highly elastic Ecoflex substrate based on a simple and accurate two-step contact-transfer patterning technique. The υCNT conductors showed reliable mechanical and electrical performance under various even severe elastic deformations. A simple LED demonstration also revealed the feasibility of the υCNT conductors in practical use. As a potential application of a υCNT conductor, highly elastic piezocapacitive strain gauge was fabricated by employing them as stretchable parallel-plate electrodes in an elastomeric platform. The capacitive responses of the fabricated strain gauge were found to be highly linear over a wide detectable range of strains and pressures without any irreversible degradation in both mechanical and electrical functionalities. In addition, no hysteretic behavior in the strain gauge was observed, even when other types of deformations (twisting, bending, and folding) were imposed on the device. After mounting the strain gauge on the joint regions of the finger and knee, the large-scale static and dynamic motions of the body parts were successfully monitored in real time, indicating potential for diverse applications where the detection of high levels of strain deformations is needed.

Acknowledgements

This research was supported by the Basic Science Research Program through the National Research Foundation of Korea (NRF) funded by the Ministry of Science, ICT & Future Planning (Nos. 2012R1A1A1009444 and 2011-0014709).

Appendix A. Supplementary data

Supplementary data associated with this article can be found, in the online version, at http://dx.doi.org/10.1016/j.carbon.2014.08.079.

REFERENCES

[1] Xu S, Zhang Y, Cho J, Lee J, Huang X, Jia L, et al. Stretchable batteries with self-similar serpentine interconnects and integrated wireless recharging systems. Nat Commun 2013;4:1543.
[2] Kim D-H, Song J, Choi WM, Kim H-S, Kim R-H, Liu Z, et al. Materials and noncoplanar mesh designs for integrated circuits with linear elastic responses to extreme mechanical deformations. Proc Natl Acad Sci USA 2008;105:18675–80.
[3] Gray DS, Tien J, Chen CS. High-conductivity elastomeric electronics. Adv Mater 2004;16:393–7.
[4] Brosteaux D, Axisa F, Gonzalez M, Vanfleteren J. Design and fabrication of elastic interconnections for stretchable electronic circuits. IEEE Electron Device Lett 2007;28:552–4.
[5] Huyghe B, Rogier H, Vanfleteren J, Axia F. Design and manufacturing of stretchable high-frequency interconnects. IEEE Trans Adv Packag 2008;31:802–8.
[6] Bowden N, Brittain S, Evans AG, Hutchinson JW, Whitesides GM. Spontaneous formation of ordered structures in thin films of metals supported on an elastomeric polymer. Nature 1998;393:146–9.
[7] Lacour SP, Wanger S, Huang Z, Suo Z. Stretchable gold conductors on elastomeric substrates. Appl Phys Lett 2003;82:2404–6.
[8] Lacour SP, Jones J, Suo Z, Wagner S. Design and performance of thin metal film interconnects for skin-like electronic circuits. IEEE Electron Device Lett 2004;25:179–81.
[9] Wang X, Hu H, Shen Y, Zhou X, Zheng Z. Stretchable conductors with ultrahigh tensile strain and stable metallic conductance enabled by prestrained polyelectrolyte nanoplatforms. Adv Mater 2011;23:3090–4.
[10] Yun S, Niu X, Yu Z, Hu W, Brochu P, Pei Q. Compliant silver nanowire-polymer composite electrodes for bistable large strain actuation. Adv Mater 2012;24:1321–7.
[11] Xu F, Zhu Y. Highly conductive and stretchable silver nanowire conductors. Adv Mater 2012;24:5117–22.
[12] Lee P, Lee J, Lee H, Yeo J, Hong S, Nam KH, et al. Highly stretchable and highly conductive metal electrode by very long metal nanowire percolation network. Adv Mater 2012;24:3326–32.

[13] Ge J, Yao H-B, Wang X, Ye Y-D, Wang J-L, Wu Z-Y, et al. Stretchable conductors based on silver nanowires: improved performance through a binary network design. Angew Chem Int Ed 2013;52:1654–9.
[14] Hu W, Niu X, Li L, Yun S, Yu Z, Pei Q. Intrinsically stretchable transparent electrodes based on silver-nanowire–crosslinked-polyacrylate composites. Nanotechnology 2012;23:344002.
[15] Ho X, Tey JN, Liu W, Kweng C, Wei J. Biaxially stretchable silver nanowire transparent conductors. J Appl Phys 2013;113:044311.
[16] Kim KS, Zhao Y, Jang H, Lee SY, Kim JM, Kim KS, et al. Large-scale pattern growth of graphene films for stretchable transparent electrodes. Nature 2009;457:706–10.
[17] Chen Z, Ren W, Gao L, Liu B, Pei S, Cheng H-M. Three-dimensional flexible and conductive interconnected graphene networks grown by chemical vapour deposition. Nat Mater 2011;10:424–8.
[18] Xu Z, Liu Z, Sun H, Cao C. Highly electrically conductive Ag-doped graphene fibers as stretchable conductors. Adv Mater 2013;25:3249–53.
[19] Sekitani T, Noguchi Y, Hata K, Fukushima T, Aida T, Someya T. A rubberlike stretchable active matrix using elastic conductors. Science 2008;321:1468–72.
[20] Lee H, Yoo J-K, Park J-H, Kim JH, Kang K, Jung YS. A stretchable polymer–carbon nanotube composite electrode for flexible lithium-ion batteries: porosity engineering by controlled phase separation. Adv Energy Mater 2012;2:976–82.
[21] Chen M, Tao T, Zhang L, Gao W, Li C. Highly conductive and stretchable polymer composites based on graphene/MWCNT network. Chem Commun 2013;49:1612–4.
[22] Huang YY, Terentjev EM. Tailoring the electrical properties of carbon nanotube–polymer composites. Adv Funct Mater 2010;20:4062–8.
[23] Kim KH, Vural M, Islam MF. Single-walled carbon nanotube aerogel-based elastic conductors. Adv Mater 2011;23:2865–9.
[24] Sekitani T, Nakajima H, Maeda H, Fukushima T, Aida T, Hata K, et al. Stretchable active-matrix organic light-emitting diode display using printable elastic conductors. Nat Mater 2009;8:494–9.
[25] Liu C-X, Choi J-W. Precision patterning of conductive polymer nanocomposite using a laser-ablated thin film. J Micromech Microeng 2012;22:045014.
[26] Lu N, Lu C, Yang S, Rogers J. Highly sensitive skin-mountable strain gauges based entirely on elastomers. Adv Funct Mater 2012;22:4044–50.
[27] Shin MK, Oh J, Lima M, Kozlov ME, Kim SJ, Baughman RH. Elastomeric conductive composites based on carbon nanotube forests. Adv Mater 2010;22:2663–7.
[28] Yu Z, Niu X, Liu Z, Pei Q. Intrinsically stretchable polymer light-emitting devices using carbon nanotube-polymer composite electrodes. Adv Mater 2011;23:3989–94.
[29] Wang X, Li T, Adams J, Yang J. Transparent, stretchable, carbon-nanotube-inlaid conductors enabled by standard replication technology for capacitive pressure, strain and touch sensors. J Mater Chem A 2013;1:3580–6.
[30] Hu L, Yuan W, Brochu P, Gruner G, Pei Q. Highly stretchable, conductive, and transparent nanotube thin films. Appl Phys Lett 2009;94:161108.
[31] Lipomi DJ, Vosgueritchian M, Tee BC-K, Hellstrom SL, Lee JA, Fox CH, et al. Skin-like pressure and strain sensors based on transparent elastic films of carbon nanotubes. Nat Nanotechnol 2011;6:788–92.
[32] Cohen DJ, Mitra D, Peterson K, Maharbiz MM. A highly elastic, capacitive strain gauge based on percolating nanotube networks. Nano Lett 2012;12:1821–5.
[33] Kim TA, Lee S-S, Kim H, Park M. Acid-treated SWCNT/polyurethane nanoweb as a stretchable and transparent conductor. RSC Adv 2012;2:10717–24.
[34] Zhu Y, Xu F. Buckling of aligned carbon nanotubes as stretchable conductors: a new manufacturing strategy. Adv Mater 2012;24:1073–7.
[35] Liu K, Sun Y, Liu P, Lin X, Fan S, Jiang K. Cross-stacked superaligned carbon nanotube films for transparent and stretchable conductors. Adv Funct Mater 2011;21:2721–8.
[36] Zhang Y, Sheehan CJ, Zhai J, Zou G, Luo H, Xiong J, et al. Polymer-embedded carbon nanotube ribbons for stretchable conductors. Adv Mater 2010;22:3027–31.
[37] Zu M, Li Q, Wang G, Byun J-H, Chou T-W. Carbon nanotube fiber based stretchable conductor. Adv Funct Mater 2013;23:789–93.
[38] Wu J, Zang J, Rathmell AR, Zhao X, Wiley BJ. Reversible sliding in networks of nanowires. Nano Lett 2013;13:2381–6.